

Crystalline Silver Nanowires by Soft Solution Processing

Yugang Sun, Byron Gates, Brian Mayers, and Younan Xia*

Department of Chemistry, University of Washington, Seattle, Washington 98195-1700

Received December 4, 2001

ABSTRACT

This paper describes a soft, solution-phase approach to the large-scale synthesis of uniform nanowires of bicrystalline silver whose lateral dimensions could be controlled in the range of 30–40 nm, and lengths up to $\sim 50\ \mu\text{m}$. The first step of this procedure involved the formation of platinum nanoparticles by reducing PtCl_2 with ethylene glycol heated to $\sim 160\ ^\circ\text{C}$. Due to their close match in crystal structure and lattice constants, these platinum nanoparticles could serve as seeds for the heterogeneous nucleation and growth of silver that was produced in the solution via the reduction of AgNO_3 with ethylene glycol. When surfactants such as poly(vinyl pyrrolidone) (PVP) were present in this solution, the silver could be directed to grow into uniform nanowires with aspect ratios as high as ~ 1000 . Measurements of transport property at room temperature indicated that these nanowires were electrically continuous with a conductivity of approximately $0.8 \times 10^5\ \text{S/cm}$.

One-dimensional (1D) nanostructures of metals play an important role as both interconnects and active components in fabricating nanoscale electronic devices.¹ They also provide an ideal model system to experimentally investigate physical phenomena such as quantized conductance and localization effects.² Silver nanowires with well-defined dimensions are particularly interesting to synthesize and study because bulk silver exhibits the highest electrical (or thermal) conductivity among all metals. Silver has also been used in a rich variety of commercial applications, and the performance of silver in these applications could be potentially enhanced by processing silver into 1D nanostructures with well-controlled dimensions and aspect ratios. For instance, the loading of silver in a polymeric composite could be significantly reduced when nanoparticles of silver are replaced by nanowires having higher aspect ratios.³

A number of chemical approaches have been actively explored to process silver into 1D nanostructures. For example, silver nanowires have been synthesized by reducing AgNO_3 with a developer in the presence of AgBr nanocrystallites,⁴ or by arc discharging between two silver electrodes immersed in an aqueous NaNO_3 solution.⁵ Silver nanorods have been produced by irradiating an aqueous AgNO_3 solution with ultraviolet light in the presence of poly(vinyl alcohol).⁶ The final products of all these methods are, however, characterized by problems such as low yields, irregular morphologies, polycrystallinity, and low aspect ratios. In contrast, the template-directed synthesis offers a better controlled route to 1D silver nanostructures. A variety of templates have been successfully demonstrated for use with this process, and typical examples include channels in

macroporous membranes,⁷ mesoporous materials,⁸ or carbon nanotubes;⁹ block copolymers;¹⁰ DNA chains;¹¹ rod-shaped micelles;¹² arrays of calix[4]hydroquinone nanotubes;¹³ and steps or edges on solid substrates.¹⁴ Here we wish to report a soft (with temperatures $< 200\ ^\circ\text{C}$), solution-phase approach that allows for the production of bicrystalline nanowires of silver with uniform diameters and in bulk quantities.

The first step of our synthesis involved the formation of Pt nanoparticles by reducing PtCl_2 with ethylene glycol refluxed at $\sim 160\ ^\circ\text{C}$.¹⁵ In this so-called *polyol process*, ethylene glycol served as both solvent and reducing agent.¹⁶ When AgNO_3 and poly(vinyl pyrrolidone) (PVP) were added to this refluxing solution that contained Pt seeds, silver nanoparticles were formed immediately through the reduction of AgNO_3 by ethylene glycol.¹⁷ After the AgNO_3 solution had been added for ~ 18 min, the reaction mixture turned turbid with a gray color, and nanorods started to appear in the reaction mixture when a small portion of the solution was taken from the vessel and viewed under an optical microscope. As the reaction mixture was refluxed at $\sim 160\ ^\circ\text{C}$, the number and length of these nanorods increased over a period up to ~ 60 min.

The exact mechanism for the formation of silver nanowires via this solution-phase approach is still under investigation by our group. Here is a working hypothesis that agreed well with the electron microscopy and spectroscopy studies. Figure 1 gives the electron microscopy images of four samples that were taken from the refluxing solution after AgNO_3 and PVP had been added for different periods of time: (A) 10, (B) 20, (C) 40, and (D) 60 min. These images indicate the evolution of silver into nanostructures having different morphologies as the reaction mixture was kept

* Corresponding author. E-mail: xia@chem.washington.edu.

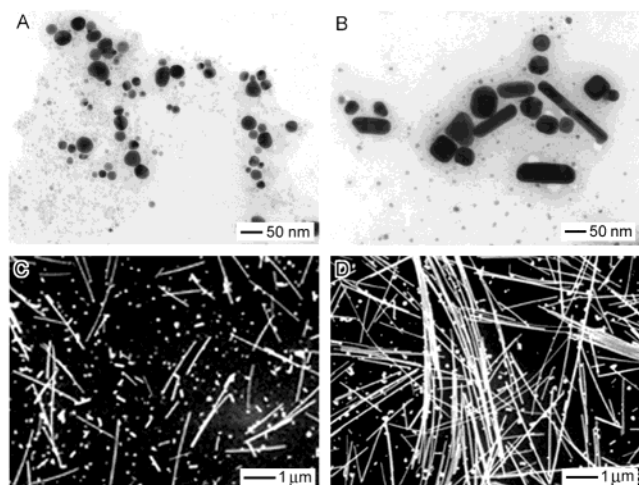


Figure 1. (A, B) TEM and (C, D) SEM images of four as-synthesized samples of silver nanowires, showing different stages of wire growth. The sample was prepared by taking a small portion of solution from the reaction mixture after AgNO_3 and PVP had been added for (A) 10, (B) 20, (C) 40, and (D) 60 min. The solution was placed on a TEM grid to let the solvent slowly evaporate in a fume hood.

refluxing at $\sim 160^\circ\text{C}$. When AgNO_3 was reduced by ethylene glycol in the presence of PVP, the initial product was a mixture of silver nanoparticles with two major distinctive sizes (Figure 1A): most of them were < 5 nm in diameter that were formed in the solution through a homogeneous nucleation process, while some of them were 20–30 nm in diameter that were formed through heterogeneous nucleation on the platinum seeds. These silver nanoparticles were prevented from aggregation into larger ones due to the presence of PVP macromolecules that could chemically absorb onto the surfaces of silver nanoparticles.¹⁸ When this colloidal dispersion was constantly refluxed at $\sim 160^\circ\text{C}$, the small silver nanoparticles started to dissolve into the solution and grow onto large nanoparticles of silver via a process known as Ostwald ripening.¹⁹ With the assistance of PVP, these large silver nanoparticles were able to grow into rod-shaped structures as shown in Figure 1B. The exact role of PVP in this process is still not clear. One possible function for PVP was to kinetically control the growth rates of various faces by interacting with these faces through adsorption and desorption.²⁰ The slow dissolution of the small silver particles into the solution might also play a certain role in achieving an anisotropic growth for the large silver particles. In principle, this growth process would continue until all silver particles with diameters < 5 nm had been completely consumed (Figures 1C and 1D). Note that some silver particles did not develop into the rod-shaped structures (Figure 1B) and kept growing into larger colloids that were as stable as the wires. These particles could coexist in the solution with the silver wires (Figure 1D). Both platinum seeds and PVP were critical to the formation of silver nanowires: no wire was generated without the addition of PtCl_2 or PVP to the reaction mixture.

Figure 2 shows the UV–visible absorption spectra taken from the solutions that were used for electron microscopy

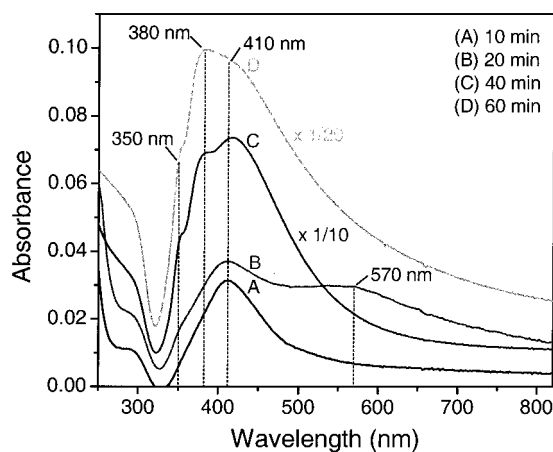


Figure 2. UV–vis absorption spectra of the reaction mixture after AgNO_3 and PVP were added for (A) 10, (B) 20, (C) 40, and (D) 60 min. All these solutions were diluted by 30 times of water before taking spectra. The absorptions at 350, 380, 410, and 570 nm were attributed to the plasmon resonance peaks of silver with various origins: long nanowires similar to the bulk silver, transverse mode of nanowires or nanorods, surface plasmon of nanoparticles, and the longitudinal mode of nanorods.

studies in Figure 1. The change in optical features observed in these spectra correlates well with the electron microscopy images. At $t = 10$ min, the appearance of a weak plasmon peak at ~ 410 nm indicated the formation of silver nanoparticles with diameters of 20–30 nm and at a relatively low concentration.²¹ The intensity of this plasmon peak changed very little until ~ 20 min into the reaction when a new peak developed at ~ 570 nm. This new peak could be attributed to the longitudinal plasmon resonance of rod-shaped silver nanostructures.²² As the length of these nanorods grew with time, the transverse plasmon mode (at ~ 380 nm) was greatly increased in intensity (note the scale change between curves B and C), while the longitudinal plasmon resonance essentially disappeared. At the same time, optical signatures similar to those of bulk silver started to appear, as indicated by a shoulder around 350 nm which could be attributed to the plasmon resonance of bulk silver film. As the reaction proceeded, the two plasmon peaks at 380 and 350 nm were further increased in intensity relative to the plasmon peak positioned at 410 nm. Nevertheless, the peak around 410 nm (this peak slightly shifted to longer wavelengths as the particles grew in size) still existed, even after the reaction mixture had been refluxed for 60 min or longer. This observation indicates that the final product synthesized under this particular condition was a mixture of silver nanowires and nanoparticles (Figure 1D).

The silver nanowires could be separated from the nanoparticles using centrifugation. In this case, the reaction mixture was cooled to room temperature, diluted with acetone (about 10 times by volume), and centrifuged at 2000 rpm for 20 min. The nanowires settled down to the bottom of the container under centrifugation while the nanoparticles that still remained in the liquid phase were removed using a pipet. This separation procedure was repeated several times until nanowire samples essentially free of particles were

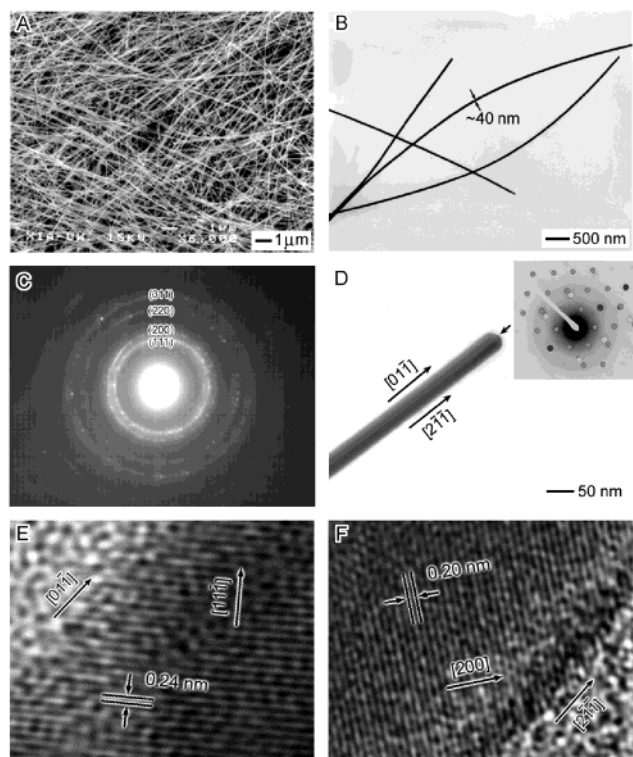


Figure 3. (A, B) SEM and TEM images of silver nanowires that were separated from a product containing silver nanoparticles through centrifugation. (C) The SAED pattern obtained from a bundle of silver nanowires randomly deposited on the TEM grid. (D) The TEM image of a silver nanowire, showing the bicrystallinity and corresponding growth directions that are characteristics of silver nanowires synthesized using the present method. The $[111]$ twin plane in the middle of this nanowire is indicated by an arrow. The inset gives the microdiffraction pattern recorded by focusing the electron beam (with a diameter of ~ 40 nm) onto this wire, with the red-colored spots indexed to the $[2\bar{1}\bar{1}]$ growth direction, and the green-colored spots to the $[01\bar{1}]$. The blue spots are shared by the two different sides of this twinned crystal. (E, F) High-resolution TEM images taken from each edge of this bicrystalline nanowire of silver, indicating the single crystallinity of each side.

obtained. Figure 3A shows the SEM image of silver nanowires after three cycles of centrifugation/separation. These nanowires had a mean diameter of ~ 38 nm, with a standard deviation of ~ 5 nm. Figure 3B shows the TEM image of several such nanowires, indicating the uniformity in diameter along each wire. Figure 3C shows the selected area electron diffraction (SAED) pattern obtained from a massive bundle of silver nanowires. All of these diffraction rings could be indexed to face-center-cubic silver, with a lattice constant of ~ 4.08 Å. The X-ray diffraction (XRD) pattern taken from a larger quantity of sample also suggested that silver nanowires synthesized using this solution-phase method existed purely in the face-center-cubic phase. The crystal structures of these silver nanowires were further studied using electron microdiffraction and high-resolution TEM. Previous studies have suggested a low threshold for twinning parallel to the $\{111\}$ faces for face-center-cubic metals such as silver and gold.²³ They tend to grow as bicrystals twinned at $\{111\}$ planes. Figure 3D shows the TEM image of the end of a silver nanowire, clearly showing

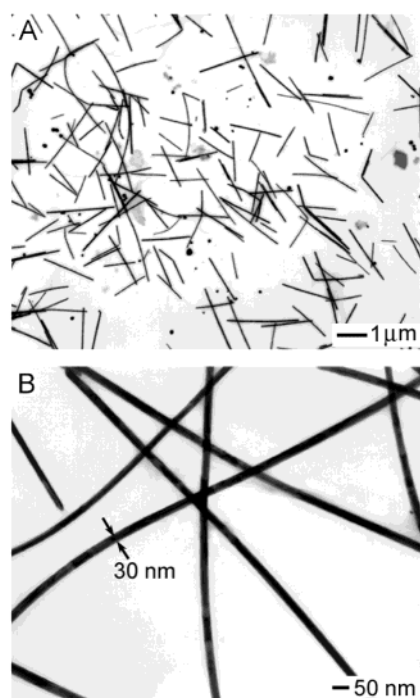


Figure 4. TEM images of two as-synthesized samples of silver nanowires, showing the variation of wire dimensions when reaction conditions were changed. These two samples were prepared using a procedure similar to that of Figures 1–3, except that (A) the ethylene glycol was refluxed at 185 °C when AgNO_3 and PVP were added, and (b) the concentration of PtCl_2 was increased by 10 times.

the $[111]$ twin plane parallel to its longitudinal axis. The inset gives the electron diffraction pattern obtained by focusing the electron beam (~ 40 nm in diameter) onto this nanowire. The assignment of this pattern suggests $[2\bar{1}\bar{1}]$ and $[01\bar{1}]$ as the growth directions for these two twinned regions, respectively. The HRTEM images shown in Figures 3E and 3F indicate that each portion of this twinned nanowire was single crystalline, each with a well-resolved interference fringe spacing.

The dimensions of these bicrystalline silver nanowires were found to strongly depend on the reaction conditions such as temperature and the concentration of the seeding solution. When the reaction temperature was higher or lower than 160 °C, the lengths of silver nanowires decreased significantly (from ~ 50 to ~ 2 μm). Very few silver nanowires were formed if the reaction temperature was lower than 100 °C. Figure 4A shows the TEM image of relatively short nanowires (nanorods) of silver that were grown at ~ 185 °C. These nanorods had a mean diameter of 39 ± 3 nm and average length of 1.9 ± 0.4 μm . Figure 4B shows the TEM image of a sample that was synthesized using a procedure similar to that used for the sample shown in Figure 3, except that the concentration of PtCl_2 was increased by 10 times. In this case, the diameter of these silver nanowires was reduced from ~ 40 to ~ 30 nm due to an increase in seed number. These experimental results suggest that it would be possible to control the dimensions of silver nanowires by varying the experimental conditions.

We have tested the electrical continuity of these silver nanowires by measuring the resistance of an individual nanowire at room temperature using the four-probe method. In this case, a silver nanowire of ~ 40 nm in diameter and ~ 20 μm in length was aligned across four gold electrodes that had been patterned on a glass slide. Currents were measured as a range of DC voltages that were applied to these gold electrodes. A linear I – V curve was obtained, from which an electrical conductivity of $\sim 0.8 \times 10^5$ S/cm was calculated for this nanowire. This value is very reasonable for such a thin nanowire (the conductivity of bulk silver is 6.2×10^5 S/cm), and strongly indicates that the bicrystalline nanowires of silver synthesized using the present chemical approach are electrically continuous.

In summary, we have demonstrated a practical approach to the large-scale synthesis of silver nanowires that have uniform diameters in the range of 30–40 nm and lengths up to ~ 50 μm . In this process, the evolution of silver into anisotropic nanostructures within an isotropic medium was determined mainly by two factors: (i) the formation of platinum seeds in the solution that could effectively separate the subsequent nucleation and growth steps of silver; (ii) the use of a polymer surfactant that could kinetically control the growth rates of various planes of face-center-cubic silver. Since the polyol process we used here has been previously applied to the synthesis of colloidal particles from a broad range of metals,²⁴ we believe the approach we demonstrated here could also be extended to these metals. The only requirement seems to be the selection of a proper seeding solid and an appropriate polymer surfactant that could chemically absorb onto the surfaces of these metals.

Acknowledgment. This work has been supported in part by the ONR, a Fellowship from the David and Lucile Packard Foundation, and a Research Fellowship from the Alfred P. Sloan Foundation. B.G. and B.M. thank the Center for Nanotechnology at the UW for the IGERT fellowship funded by the NSF (DGE-9987620). We also thank Mrs. Yu Lu, Mr. Yadong Yin, Mr. Hanson Fong, and Dr. Brian Reed for their help with XRD, electron microdiffraction, and HRTEM studies.

References

- (a) Prokes, S. M.; Wang, K. L. *MRS Bull.* **1999**, 24(8), 13. (b) Cui, Y.; Wei, Q.; Park, H.; Lieber, C. M. *Science* **2001**, 293, 1289.
- (a) Hu, J.; Odom, T. W.; Lieber, C. M. *Acc. Chem. Res.* **1999**, 32, 435. (b) Zhang, Z.; Sun, X.; Dresselhaus, M. S.; Ying, J. Y. *Phys. Rev. B* **2000**, 61, 4850. (c) Bockrath, M.; Liang, W.; Bozovic, D.; Hafner, J. H.; Lieber, C. M.; Tinkham, M.; Park, H. *Science* **2001**, 291, 283.
- Carmona, F.; Barreau, F.; Delhaes, P.; Canet, R. *J. Phys. Lett.* **1980**, 41, L-531.
- Liu, S.; Yue, J.; Gedanken, A. *Adv. Mater.* **2001**, 13, 656.
- Zhou, Y.; Yu, S. H.; Cui, X. P.; Wang, C. Y.; Chen, Z. Y. *Chem. Mater.* **1999**, 11, 545.
- Zhou, Y.; Yu, S. H.; Wang, C. Y.; Li, X. G.; Zhu, Y. R.; Chen, Z. Y. *Adv. Mater.* **1999**, 11, 850.
- See, for example, (a) Martin, C. R. *Science* **1994**, 266, 1961. (b) Martin, B. R.; Dermody, D. J.; Reiss, B. D.; Fang, M.; Lyon, L. A.; Natan, M. J.; Mallouk, T. E. *Adv. Mater.* **1999**, 11, 1021. (c) Zhang, Z.; Gekhtman, D.; Dresselhaus, M. S.; Ying, J. Y. *Chem. Mater.* **1999**, 11, 1659.
- (a) Han, Y. J.; Kim, J. M.; Stucky, G. D. *Chem. Mater.* **2000**, 12, 2068. (b) Huang, M. H.; Choudrey, A.; Yang, P. *Chem. Commun.* **2000**, 1063.
- (a) Ajayan, P. M.; Iijima, S. *Nature* **1993**, 361, 333. (b) Ugarte, D.; Chatelain, A.; de Heer, W. A. *Science* **1996**, 274, 1897.
- Zhang, D.; Qi, L.; Ma, J.; Cheng, H. *Chem. Mater.* **2001**, 13, 2753.
- Braun, E.; Eichen, Y.; Sivan, U.; Ben-Yoseph, G. *Nature* **1998**, 391, 775.
- (a) Jana, N. R.; Gearheart, L.; Murphy, C. J. *Chem. Commun.* **2001**, 617. (b) El-Sayed, M. A. *Acc. Chem. Res.* **2001**, 34, 257.
- Hong, B. H.; Bae, S. C.; Lee, C.-W.; Jeong, S.; Kim, K. S. *Science* **2001**, 294, 348.
- (a) Song, H. H.; Jones, K. M.; Baski, A. A. *J. Vac. Sci. Technol. A* **1999**, 17, 1696. (b) Zach, M. P.; Ng, K. H.; Penner, R. M. *Science* **2000**, 290, 2120.
- In a typical synthesis, 2×10^{-5} g of PtCl_2 (Aldrich, 99.99+%) was dissolved into 0.5 mL ethylene glycol (Aldrich, 99.8%), and this solution was added to 5 mL ethylene glycol (heated to 160 °C) under continuous magnetic stirring. After ~ 4 min, 2.5 mL ethylene glycol solution of AgNO_3 (0.0500 g, Aldrich, 99+%) and 5 mL ethylene glycol solution of poly(vinyl pyrrolidone) (PVP, 0.200 g, Aldrich, $M_w \approx 40\,000$) were added to the ethylene glycol containing platinum seeds. This reaction mixture was then constantly heated at 160 °C for various periods of time up to ~ 60 min. The nanowires were separated from particles using centrifugation. In this case, the reaction mixture was cooled to room temperature, diluted with acetone (about 10 times by volume), and centrifuged at 2000 rpm for 20 min. The nanowires settled down to the bottom of the container under centrifugation while the nanoparticles that still remained in the liquid phase were removed using a pipet. This separation procedure was repeated several times until nanowire samples essentially free of particles were obtained. The SEM images were obtained on a field emission microscope (FSEM, JEOL-6300F, Peabody, MA) operating at an accelerating voltage of 15 kV. The TEM images and microdiffraction patterns were taken on a JEOL-1200EX II microscope (80 kV). High-resolution TEM images were obtained on a TOPCON 002B microscope operated at 160 kV. XRD measurements were obtained with a Philips PW1710 diffractometer (Cu–K α radiation).
- Fievet, F.; Lagier, J. P.; Figlarz, M. *MRS Bull.* **1989**, December, 29.
- Ayyappan, S.; Subbanna, G. N.; Gopalan, R. S.; Rao, C. N. R. *Solid State Ionics* **1996**, 84, 271.
- Zhang, Z.; Zhao, B.; Hu, L. *J. Solid State Chem.* **1996**, 121, 105.
- Roosen, A. R.; Carter, W. C. *Physica A* **1998**, 261, 232.
- Bonet, F.; Tekaiia-Elhsissen, K.; Sarathy, K. V. *Bull. Mater. Sci.* **2000**, 23, 165.
- Kerker, M. J. *Colloid Interface Sci.* **1985**, 105, 297.
- Dickson, R. M.; Lyon, L. A. *J. Phys. Chem. B* **2000**, 104, 6095.
- (a) Bögel, G.; Meekes, H.; Bennema, P.; Bollen, D. J. *Phys. Chem. B* **1999**, 103, 7577. (b) Link, S.; Wang, Z. L.; El-Sayed, M. A. *J. Phys. Chem. B* **2000**, 104, 7867.
- Viau, G.; Fievet-Vincent, F.; Fievet, F. *Solid State Ionics* **1996**, 84, 259.

NL010093Y